In Situ Surface Enhanced Raman Spectroscopy on Electrodes with Platinum and Palladium Nanoparticle Ensembles

Roberto Gómez, Juan M. Pérez,* José Solla-Gullón, Vicente Montiel, and Antonio Aldaz

Departament de Química Física and Institut Universitari d'Electroquímica, Universitat d'Alacant, Apartat de correus 99, E-03080 Alacant, Spain

Received: December 29, 2003; In Final Form: April 20, 2004

In situ Raman spectra have been obtained for different species (CN^-, CO, H) adsorbed on nanostructured electrodes prepared by deposition of pure Pt and Pd nanoparticles (around 4 nm in size) on either gold or platinum electrodes in acidic solutions. The surface enhancement factor has been estimated on the basis of cyanide spectra obtained both at the surface and in solution. It attains a value as high as 550, around 3−4 times higher than that reported for roughened Pt electrodes for the same adsorbate. In the case of CO, typical bands for the stretching of the Pt/Pd−C and C−O bonds have been observed for low acquisition times (ca. 1 s), evidencing that pure Pt and Pd nanoparticles sustain significant surface enhancement effects. The spectra show mainly atop CO coordination for Pt nanoparticles whereas both linear and bridge CO are detected for Pd nanoparticles. The potential advantages of the nanoparticle-on-electrode approach in Raman spectroelectrochemical studies are highlighted.

Introduction

Since the first report by Fleishmann in 1974,[1] the popularity of surface enhanced Raman spectroscopy steadily increased due to its wide applicability. Innovative and extensive analytical applications can be found in several fields, such as surface science,[2] electrochemistry,[3,4] biology,[5,6] and materials science.[7] There exist excellent revisions on this subject,[8,9] the most recent being that authored by Tian.[10] More specifically, it is worth noting that SERS is a viable tool, capable of adaptation for in situ investigations in the field of heterogeneous catalysis.[11] Among the different subjects of research, emphasis has been put on the application of SERS to problems of electrochemical significance (detection of adsorbates under reactive and unreactive conditions, interfacial structure,[12] electropolymerization,[13]...). Initially, the technique was restricted to electrodes of Ag, Au, and Cu with surfaces roughened through electrochemical oxidation−reduction cycles (ORC) although pioneering works also appeared for Pt electrodes.[14,15] Interest in electrocatalysis triggered an important effort toward a more systematic extension of the technique to platinum-group metals. Initially the strategy followed consisted of preparing ultrathin layers (1−3 monolayers) of the catalytic metals on roughened Au.[16] Later, it was demonstrated that appropriate roughening of Pt-group metals by ORCs also led to a significant (albeit admittedly modest) enhancement effect.[17] Very recently, UV−SERS of molecules adsorbed at rough Rh and Ru metal surfaces have been obtained.[18]

It is generally accepted that the enhancement effect results from both electromagnetic (EM) and chemical (charge transfer, CT) mechanisms.[19] Although these mechanisms are not mutually exclusive, the use of nonflat geometries, such as islands films,[20,21] roughened electrodes,[1] encapsulated particles,[22] and particularly nanoparticle aggregates[23,24] has tended to substantiate the EM mechanism as the prevalent one[25] with a possible further contribution from the CT mechanism.

The maximum intensification has been observed for systems with features in the range of 10 to 100 nm: roughness obtained by ORC, thin films obtained by evaporation and sputtering, colloids, ... One feasible approach consists of depositing transition-metal (Au, Cu, Ag) nanoparticles (spontaneous deposition) on a substrate inactive for SERS (nonroughened metal, graphite, etc.), which is sometimes known as the nanoparticles-on-electrode approach.[26,27] This approach has been successfully employed for closely related Fourier transform infrared spectroscopy studies.[28] Along these lines, one of the aspects that is attracting increasing attention nowadays is the electrocatalytic activity of nanoparticles.[29] Obviously, the application of SERS to electrodes composed of a thin layer of nanoparticles could open new prospects in the investigation of their adsorptive and electrocatalytic behavior, especially regarding the detection and identification of poisons and intermediates. A first report with Pt and Pd nanoparticles showing clear SER spectra for typical adsorbates, such as ethylene and CO, has appeared recently.[30] These nanoparticles were actually made of gold upon which a monolayer of either Pd or Pt was deposited and do not necessarily behave as particles of pure Pt or Pd. Undoubtedly, it would be advantageous to obtain significant SERS activity from pure transition metal (especially from Pt-group metals) nanoparticles. In this respect, electrocatalytic research combined with SERS studies have been performed with pure iron nanoparticles.[27] On the other hand, Tian and co-workers[31] have reported important SERS activity for transition metal nanowire arrays. In this report, we extend for the first time SERS studies to the more general case of pure nanoparticles of Pt and Pd deposited randomly at a conducting substrate.

Experimental Section

Platinum and palladium nanoparticles were synthesized by means of water-in-oil microemulsions and have an average diameter of 4 nm. Subsequently, they were deposited from an

* Address correspondence to this author. Fax: (+34)96-590-3537. E-mail: jmpm@ua.es.

10.1021/jp038030m CCC: $27.50
Published on Web 06/03/2004

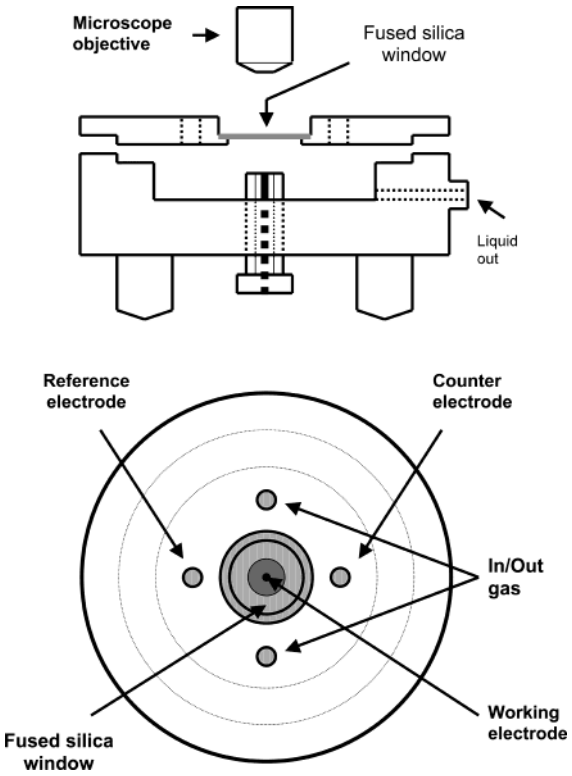

Figure 1. Sketch of the spectroelectrochemical cell for the confocal microprobe Raman system.

aqueous suspension (0.11 μg of Pd/μL and 0.34 μg of Pt/μL) via a pipet onto a disk of polycrystalline polished gold or platinum (3 and 2 mm in diameter, respectively) sheathed in a threaded PTFE piece. The (0001) face of highly oriented pyrolytic graphite, HPOG, was also used as substrate for the nanoparticles. The droplet volume used in all cases varied from 3 to 5 μL. The droplet was dried by Ar flow for ca. 5 min. This substrate was then mounted on an electrochemical PTFE cell designed to acquire in situ Raman spectra (Figure 1). A fused silica window separated the microscope objective from the electrolytic solution, which was either 0.1 M $HClO_4$ or 0.1 M H_2SO_4. A Pt wire was used as a counter electrode, whereas a saturated calomel electrode (SCE) was used as reference electrode contacting the working solution through a Luggin capillary. The nanoparticles were cleaned in the electrochemical cell either through incipient hydrogen evolution reaction or by repeating two or three cycles of CO adsorption/oxidation.[32] Raman spectra were obtained with a LabRam spectrometer (from Jovin-Yvon Horiba). The slit and pinhole employed were 200 or 300 μm and 500 or 600 μm, respectively. The excitation line was provided by a 17 mW He−Ne laser at 632.8 nm. The laser beam was focused through a 50× long-working distance objective (0.5 NA) into a 2-μm spot at the electrode surface. The spectrometer resolution was better than 3 cm^{-1} and the detector was a Peltier cooled charge-couple device (CCD) (1064 × 256 pixels). Acquisition times varied from 1 to 180 s. All the spectroscopic experiments about the adsorption of carbon monoxide were done with saturated monolayers of CO formed upon contact of the nanoparticulate electrode with a CO-saturated working solution. All the spectra shown in this paper are as obtained; no further manipulation (baseline correction, smoothing, ...) was applied.

Carbon monoxide (N47) was supplied by Air Liquide. Working solutions were prepared with ultrapure water (Millipore MiliQ) and Merck Suprapur $HClO_4$ and H_2SO_4 (concentrated solutions) or Merck (p.a.) KNO_3. Sodium cyanide supplied by Merck (p.a.) was used without further purification.

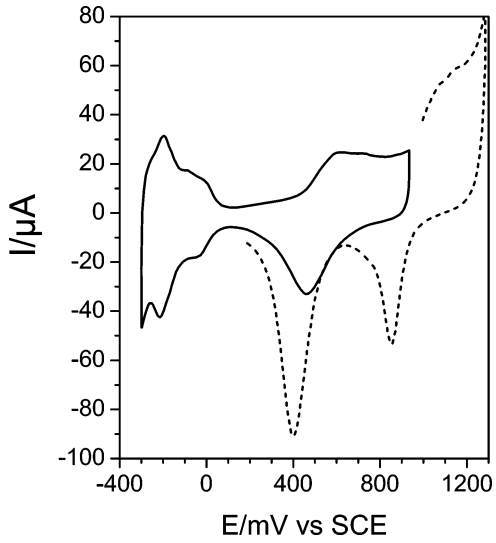

Figure 2. Voltammetric profile of a Pt_{nano}/Au electrode obtained in the spectroelectrochemical cell. The solid line corresponds to the stationary cyclic voltammogram showing the typical regions of adsorption of hydrogen and oxygen on platinum. The broken line shows the profile after opening up the potential window. Working electrolyte: 0.1 M $HClO_4$. Sweep rate: 50 mV s^{-1}. Electrode: 3 μL of a 0.34 μg/μL of Pt dispersion on a 3-mm-diameter polished gold disk.

Results and Discussion

Voltammetric Characterization. To check the cleanliness of both the spectroelectrochemical cell and, specifically, that of the deposited nanoparticles, in situ blank voltammograms were obtained. Concretely, Figure 2 corresponds to the voltammetric response of the polished gold electrode covered by platinum nanoparticles in contact with a 0.1 M $HClO_4$ solution. The solid line corresponds to the profile obtained in a restricted potential region. It shows adsorption waves due mainly to the adsorption/desorption of hydrogen on the Pt nanoparticles below 0.1 V. The adsorption of oxygenated species occurs at potentials more positive than 0.50 V in the positive-going sweep. The corresponding reduction peak is centered at 0.45 V. This profile resembles closely that obtained for a conventional and clean polycrystalline platinum electrode under the same conditions, which attests to the validity of the employed procedures. No particular effect due to the size of the particles could be observed, which is probably linked to the actual structure of the deposit. Opening the window up to 1.3 V leads to the oxidation of the Au substrate as reflected in a broad contribution (with shoulders at 1.06 and 1.15 V) in the positive-going sweep together with a well-defined reduction peak at 0.85 V. On the other hand, the peak for the reduction of the oxygenated species adsorbed on the Pt nanoparticles now appears at 0.40 V. It should be mentioned that the electrochemical response (exchanged charge) for adsorption/desorption processes such as the adsorption of hydrogen is directly proportional to the mass of particles deposited.[28] However, not all the adsorption sites available at the surface of the nanoparticles are active as part of the surface is lost by interaction with the substrate and by aggregation of the deposited nanoparticles.

Figure 3a corresponds to the voltammetric profile obtained for a polished platinum electrode upon which palladium particles were deposited. The observed behavior is clearly dominated by the presence of the Pd nanoparticles. In fact, for negative potentials, we distinguish waves corresponding both to the

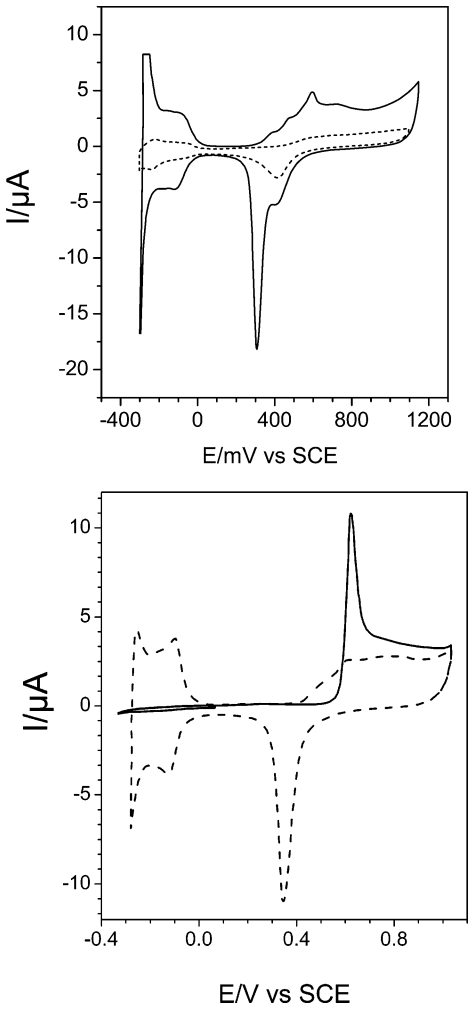

Figure 3. (a) Stationary voltammetric profile of a Pd_{nano}/Pt electrode obtained in the spectroelectrochemical cell. (Dashed line) Blank voltammogram for the bare Pt disk. Working electrolyte: 0.1 M $HClO_4$. Sweep rate: 50 mV s^{-1}. Electrode: 3 μL of a 0.11 μg/μL of Pd dispersion on a 2-mm-diameter polished platinum disk. (b) (Solid line) Voltammetric scan for the oxidation of CO adsorbed on a Pd_{nano}/Au electrode. (Dashed line) Stationary voltammetric profile for the Pd_{nano}/Au electrode obtained after CO stripping. Working electrolyte: 0.1 M H_2SO_4. Sweep rate: 50 mV s^{-1}. Electrode: 3 μL of a 0.11 μg/μL of Pd dispersion on a 3-mm-diameter polished gold disk.

adsorption and to the absorption of hydrogen at the particles, being the contribution of the platinum substrate virtually indiscernible. However, in the oxygen potential region (negative-going scan) the reduction of oxygenated species adsorbed on the Pt substrate sites can be distinguished as a shoulder located at 0.40 V. It is worth noting that the small peak appearing in the positive-going sweep at 0.60 V is linked to the oxidation of small amounts of CO adsorbed during the excursion to negative potential values. This voltammogram was obtained once CO had been mostly purged from the working solution.

Figure 3b shows a representative voltammetric profile corresponding to the stripping of a saturated CO layer adsorbed at the Pd nanoparticles supported on a gold electrode (solid line). A complete blockage of the Pd surface adsorption sites can be deduced from the removal of the typical voltammetric features in the low potential range due to the adsorption/desorption of hydrogen and anions on palladium. The subsequent voltammogram (dashed line) shows the recovery of the aforementioned contributions together with the adsorption/desorption of oxygenated species in the high potential range. The charge exchanged

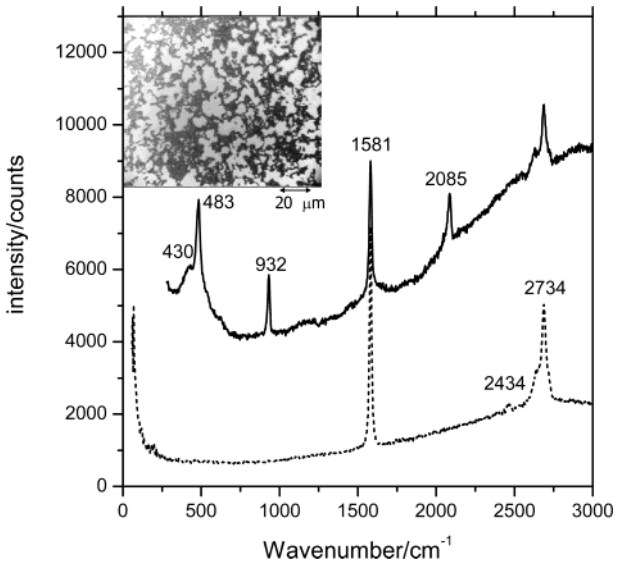

Figure 4. (Broken line) Raman spectra for the basal plane of HOPG obtained in air. (Solid line) SERS spectra obtained for CO adsorbed on Pt_{nano}/HOPG(0001) in contact with 0.1 M $HClO_4$ saturated with CO. Acquisition time: 60 s. Inset: Microscope reflection image for the aggregates of Pt nanoparticles (dark regions) on the HOPG basal plane.

during the oxidative stripping of CO on both Pt and Pd nanoparticles is fully compatible with the charge exchanged in the hydrogen potential region,[28] which indicates that the number of active surface sites at the nanoparticles is the same for H and CO adsorbates.

In Situ Raman Spectra for CO Adlayers on Pt and Pd. One question that should be discussed prior to the presentation of the spectroelectrochemical measurements is the actual existence of intrinsic SERS activity coming from the deposited particles, which should be independent of their substrate. To check this, a HOPG cleaved basal plane sample was used as a fully inactive substrate for the metallic nanoparticles. Figure 4 (dashed line) shows the Raman spectrum obtained in air at room temperature for the HOPG sample (basal plane) showing (at 1581 cm^{-1}) one of the two E_{2g} Raman-active vibrational modes of the single crystals belonging to D_{6h} symmetry. The spectrum also exhibits 2nd order features at 2434 and 2734 cm^{-1}.[33]

A droplet (5 μL) of the Pt-nanoparticle aqueous suspension (0.34 μg of Pt/μL) was attached to the surface and dried in air, allowing for deposition of the nanoparticles. The original suspension is not fully transparent (light-scattering) and shows gray/black color (dispersion), which attests to the formation of nanoparticle aggregates. The tendency to agglomerate is also observed in the deposit microstructure. Figure 4 (inset) corresponds to a reflection optical microscopy image acquired immediately after the deposition process. The dark regions correspond to parts of the surface covered by agglomerates of Pt nanoparticles whereas the regions appearing in light gray correspond to regions where no substantial deposition took place. On the basis of the area covered by the deposit, the total amount of platinum deposited, and the mean size of the particle, one can estimate that the dark regions contain as an average the equivalent to five layers of Pt nanoparticles.

Figure 4 (solid line) corresponds to the Raman spectrum obtained for the Pt-modified HOPG in contact with a 0.1 M $HClO_4$ solution saturated with CO. The laser beam was focused on one of the Pt agglomerates. New bands appear at 2085, 430, and 483 cm^{-1}, which are assigned to linear CO adsorbed onto Pt nanoparticles on the basis of recent observation with similar systems.[30] The one at high frequencies is associated with the

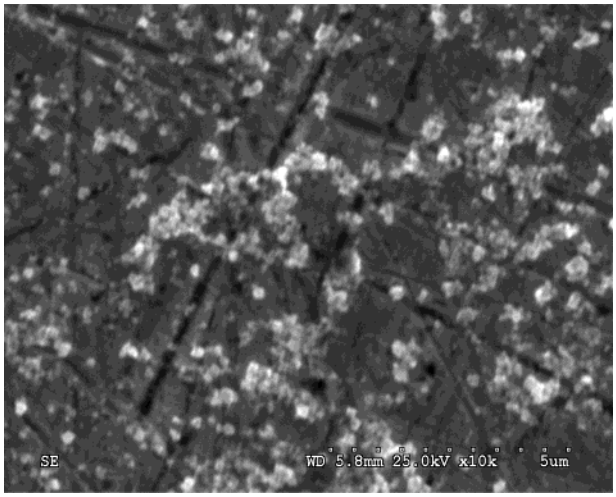

Figure 5. Scanning electron micrograph of a typical deposit of Pt nanoparticles on a polished Pt electrode.

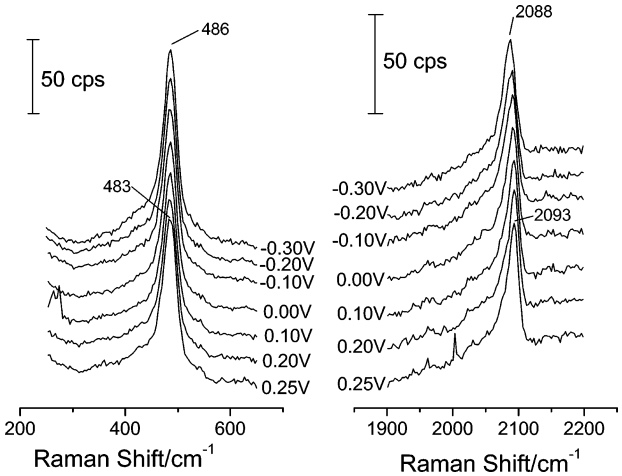

Figure 6. Series of Raman spectra for CO adsorbed on Pt nanoparticles. Potential is indicated alongside. Electrode: 3 μL of a 0.34 μg/μL of Pt dispersion on a 2-mm-diameter polished platinum disk. Working electrolyte: 0.1 M $HClO_4$ saturated with CO. Acquisition time: 60 s.

stretching of the CO bond (ν_{CO}) while the two at low frequencies are ascribed to the Pt−C stretching frequency (ν_{PtC}). The existence of two discernible Pt−C stretching features points to the existence of at least two different types of atop CO, which is not unexpected for such a substrate. The band at 430 cm^{-1} should not be ascribed to bridge-bonded CO because its corresponding band has been reported to appear at significantly lower wavenumbers (390 cm^{-1}).[16a] The band at 932 cm^{-1} corresponds to the totally symmetric stretching of interphasial and solution perchlorate (the same band appears if the excitation laser beam is focused into the solution phase). Overall, the result shown in Figure 4 attests to the existence of a significant surface enhancement coming from the Pt aggregates, since otherwise bands corresponding to adsorbates such as CO could not be discerned.

Figure 5 corresponds to a scanning electron micrograph showing the actual structure (particle distribution) of an electrode prepared by deposition of Pt nanoparticles on a polished platinum disk. It should be emphasized that using a metal substrate (Au or Pt) leads to a lower degree of nanoparticle aggregation as can be deduced through comparison of Figures 4 (inset) and 5.

Figure 6 corresponds to a series of spectra obtained for an electrode prepared by deposition of Pt nanoparticles on a platinum-polished electrode in contact with a CO-saturated perchloric acid solution at different potentials. The expected bands for the Pt−C stretching and the C−O stretching are observed respectively in the low and high wavenumber regions shown in the figure. The ν_{PtC} band intensity slightly depends on potential: the more negative, the higher the band intensity. Dependence of SERS intensity with applied potential has been observed in many cases and has been attributed to a charge-transfer (chemical) enhancement model.[34] This model assumes that the Raman intensity reaches a maximum when the energy of the exciting radiation is in resonance with a metal/adsorbate charge-transfer transition, being the energies of donor and acceptor electronic states are dependent on applied potential.

In agreement with previous studies, there is a downward shift of the frequencies of the corresponding ν_{PtC} as the potential is made more positive whereas the ν_{CO} band shifts toward higher values. It is noteworthy that $d\nu/dE$ is significantly smaller than in the case of Pt overlayers on electrochemically roughened Au surfaces.[35] For our samples, $d\nu/dE$ for ν_{PtC} and ν_{CO} can be evaluated as −5 and 9 cm^{-1} V^{-1}, respectively, whereas values reported for atop CO on Pt overlayers on gold display corresponding values of −9 and 30 cm^{-1} V^{-1}. The reasons underlying this behavior are being currently investigated in our laboratory, but they are certainly linked to the nanoparticulate structure of the electrode employed here.

It is certainly interesting to compare other spectral features present here with those typical of other Pt surfaces (i.e. thin Pt films on roughened gold[36] and Pt-covered gold nanoparticles[30]). It is remarkable that for our samples, bridge-bonded CO contributions are absent, which is in contrast with the behavior typical of the other (above-mentioned) platinum samples. The latter show sizable bands for brigde-bonded CO, maybe due to the influence of the underlying gold substrate, partially exposed to the working electrolyte. These complications are absent in our case as the nanoparticles are fully made of Pt (and are supported on a platinum disk). Another subtle difference lies in the band wavenumbers of the stretching bands at a fixed value for the applied potential. Significantly, in our case the bands appear at least 5 to 10 cm^{-1} at higher wavenumbers. Interestingly, the half width of the bands presented here (around 25 cm^{-1}) is also lower. Only the Pt-covered Au nanoparticles show a similar bandwidth for the ν_{CO} band, albeit a broader band for the Pt−C stretching. This probably reflects the relatively narrow size distribution of the Pt nanoparticles.[32] These differences could also be related to the size of the nanoparticles since, in the case of the thin films on roughened gold, the features are in the range of 100 nm and the Pt-covered gold nanoparticles are significantly larger than those used in the present report (8 vs 4 nm).

Figure 7 corresponds to spectra for CO adsorbed on Pd nanoparticles as a function of the applied potential in 0.1 M $HClO_4$. The particles were deposited on a polished Pt sample. In this case, two bands can be distinguished in both Raman shift regions. In fact, in the region of ν_{CO}, two clear-cut bands appear at 1965 and 2091 cm^{-1}, corresponding respectively to the CO-stretching in bridge- and atop-bonded CO.[30,36] Also two bands appear in the low Raman-shift region at 365 and 455 cm^{-1}, the latter being barely discernible. They correspond to the Pd−C stretching of bridge- and atop-bonded CO, respectively.[30,36] When comparing these results with other Pd surfaces, similar tendencies as in the case of Pt are confirmed. Again, the ν_{CO} bands in the spectra presented here are characterized by appearing at wavenumbers significantly higher than in the case of Pd thin films on roughened gold or Pd-covered gold

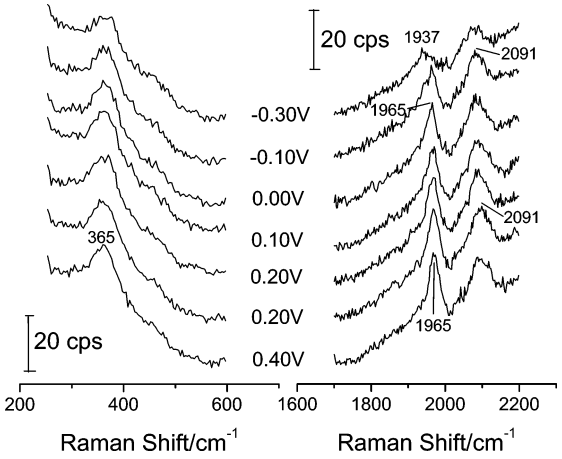

Figure 7. Series of Raman spectra for CO adsorbed on Pd nanoparticles. Potential is indicated alongside. Electrode: 3 μL of a 0.11 μg/μL of Pd dispersion on a 2-mm-diameter polished platinum disk. Working electrolyte: 0.1 M $HClO_4$ saturated with CO. Acquisition time: 60 s.

nanoparticles. In addition the dν/dE value for the CO-stretching band is again surprisingly lower than that found for other Pd samples.[30,35,36]

The possible interference of the substrate for this type of sample deserves further perusal. Pt and Pd nanoparticles supported on polished Au disk (and in contact with an acidic solution saturated with CO) yielded spectra virtually identical with those obtained by using a Pt substrate. This demonstrates the lack of influence of the substrate nature on the spectra. In addition, the adsorption of the molecule being investigated on the substrate does not seem to alter the spectra due to species adsorbed at the nanoparticles. In fact, even when the working solution is saturated with CO, the band at around 2115 cm^{-1}, typical of CO adsorbed on gold, does not appear since the polished gold electrode is fully inactive for the enhancement. In the same way, no particular enhancement seems to be induced in the surrounding gold by the nanostructured Pt or Pd deposit. However, there is still a subtle difference in the wavenumber values for the bands (they are slightly shifted with respect to the Pt substrate case) as seen in previous work on similar systems.[30,36]

In Situ Raman Spectra for H Adsorbed on Pt Nanoparticles. With the aim of exploring further the potential use of nanostructured samples prepared by spontaneous deposition as efficient substrates in SERS/electrochemical studies, we have studied the adsorption of hydrogen. Figure 8 corresponds to a series of Raman spectra obtained for a Pt electrode (Pt-nanoparticle-on-Pt) in the low potential range (near or at the hydrogen evolution potential threshold) in contact with a 0.1 M $HClO_4$ solution. As observed, together with the band due to the OH bending from water at around 1620 cm^{-1}, a weak, albeit clearly discernible, band appears at 2070 cm^{-1}. The latter only appears at sufficiently low potentials and both its position and intensity depend on potential as anticipated. From the potential values where the band appears (near or at the onset of the hydrogen evolution reaction, HER), it seems to be due to the H adatom intermediate of the HER. The results shown here clearly resemble those reported by Tian and co-workers[37] for highly roughened Pt electrodes, which evidences anew the ability of the nanostructured samples for providing remarkable and stable surface Raman enhancement.

Calculation of the Surface Enhancement Factor (G). As pointed out by Tian,[10] there is still some controversy on the existence of a significant enhancement of the Raman signal in

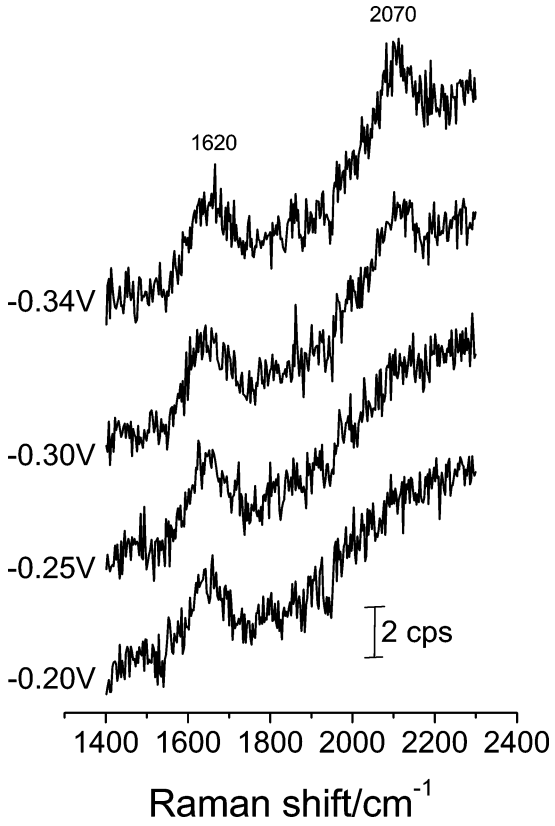

Figure 8. Series of Raman spectra for Pt nanoparticles as a function of potential (indicated alongside). Electrode: 3 μL of a 0.34 μg/μL of Pt dispersion on a 2-mm-diameter polished platinum disk. Working electrolyte: 0.1 M $HClO_4$. Acquisition time: 120 s.

the case of nanostructured Pt surfaces. In fact, the enhancement can be explained partly by an increase in the surface area, i.e., by an increase in the so-called roughness factor. However, this is not the only enhancement mechanism, since for higher roughness factors, similar or even lower band intensities have been observed for analogous systems. It is therefore convenient to calculate the enhancement factor to evidence in a non-ambiguous way the existence of the enhancement effect. In addition, given that for the first time a SERS study was performed with a nanoparticle-on-electrode approach for Pt samples, it is valuable to compare the spectra obtained here with those reported previously with surfaces prepared by electrochemical roughening of Pt massive electrodes.

The calculation of G is not easy in the case of a confocal Raman microscope such as the one used in this work, because it is difficult to evaluate the contribution from the scattering molecule in the bulk solution. However, Tian and co-workers have developed a method that can be summarized in the following expression:[38]

$$G = \frac{hcN_o\sigma I_{surf}}{RI_{bulk}} \quad (1)$$

where c, N_o, σ, and R are respectively the concentration of the Raman-active adsorbate in the bulk solution, the Avogadro constant, the surface area per adspecies, and the roughness factor of the Pt electrodes. The latter is calculated on the basis of the voltammetric charge measured in the so-called hydrogen potential region. For the electrodes employed in this work the roughness attained a value of 15. The value of h is characteristic of the confocal system[38] and in our case is about 21 μm. I_{surf} and I_{bulk} are the integrated intensities of the surface Raman signal

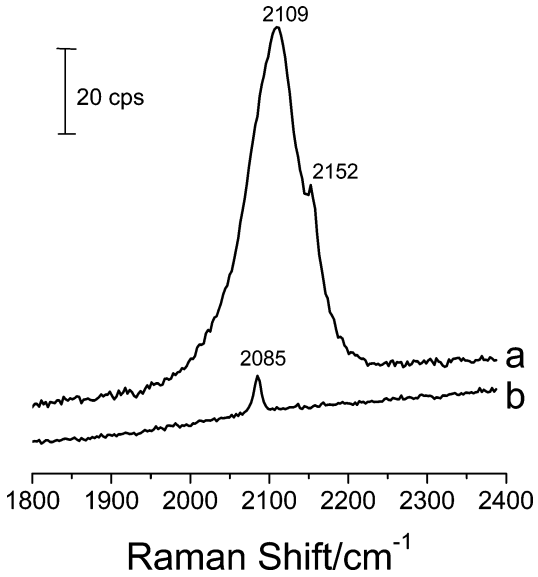

Figure 9. (a) Surface Raman spectrum for adsorbed CN^- for a Pt_{nano}/Pt electrode in contact with a 2 mM NaCN + 0.1 M KNO_3 solution. Potential: −0.4 V. Electrode: 3 μL of a 0.34 μg/μL of Pt dispersion on a 2-mm-diameter polished platinum disk. Acquisition time: 120 s. (b) Solution Raman spectrum for CN^- from a solution of 0.1 M NaCN + 0.1 M KNO_3. Acquisition time: 180 s.

for the adsorbed species and for the same species in solution, respectively.

Obviously, the calculation of G requires the choice of a species whose Raman spectrum may be easily obtainable both at the surface and in solution. In this respect we have chosen cyanide, partly because it has been the object of a very recent SERS study with a platinum substrate.[39] Figure 9a corresponds to a spectrum of CN^- adsorbed on a Pt-nanoparticle-on-Pt electrode at a potential of −0.4 V in contact with 2 mM NaCN + 0.1 M KNO_3, while spectrum b corresponds to the solution spectra for cyanide from a 0.1 M NaCN + 0.1 M KNO_3 solution. It is interesting that the spectrum for adsorbed cyanide presents a main band at 2109 cm^{-1}, which shifts clearly with potential and can be ascribed to C-end adsorbed CN^-. It is remarkable that the intensity of this band depends also on potential, its maximum being at around −0.4 V. The satellite at 2152 cm^{-1} does not shift with potential in a significant way and, according to Tian and co-workers,[39] can be ascribed to an adsorbed complex of platinum with cyanide. Overall, the spectrum shown here for adsorbed CN^- is akin to that found by the Xiamen group for roughened Pt electrodes under similar experimental conditions.

The area occupied per adsorbed cyanide is taken to be 0.0878 nm^2.[39] The integrated band intensities are 2730 cps for the adsorbed cyanide and 55 cps for the free species in solution. Equation 1 gives an enhancement factor of 550. This value is quite remarkable because it is around 3−4 times larger than the one obtained for the same system on a roughened Pt electrode. Seemingly, aggregated particles of an average diameter of 4 nm provide an unusual large enhancement.

Concluding Remarks

It has been shown that the use of the nanoparticle-on-electrode approach can be fruitfully employed for spectroelectrochemical studies in the case of pure Pt (and Pd) nanoparticles when combined with a highly sensitive instrument such as a confocal microprobe Raman system. The samples are easily prepared by deposition of the particles onto a flat metallic (Pt or Au) electrode. In fact, spectra of remarkable quality have been obtained for different adsorbed species (carbon monoxide, hydrogen, and cyanide).

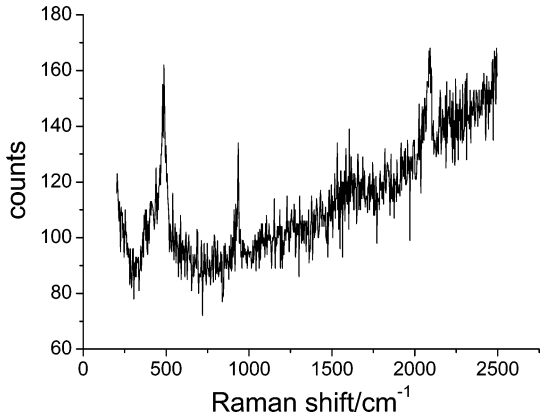

Figure 10. Surface Raman spectrum for CO adsorbed at a Pt_{nano}/Pt electrode. Potential: 0 V. Solution: 0.1 M $HClO_4$ saturated with CO. Electrode: 3 μL of a 0.34 μg/μL of Pt dispersion on a 2-mm-diameter polished platinum disk. Acquisition time: 1 s

It is worth noting that this procedure for preparing transition metal films active in SERS presents some advantages over the classical electrochemical roughening. In fact, the surface enhancement seems to be significantly higher; in the case of cyanide, the surface intensification factor attains a value as high as 550, around 3−4 times larger than those reported for electrochemically roughened Pt electrodes.[39] This represents an important advantage for experiments in dynamic electrochemistry where a minimization of the spectra acquisition time is crucial. As an example, Figure 10 shows the Raman spectrum for CO adsorbed on Pt_{nano}/Pt with an acquisition time of 1 s, which shows the typical vibrational features for the adsorbate. The feasibility of electrochemical experiments with simultaneous collection of Raman spectra is thus evidenced.

More importantly, the methodology presented here may allow a straightforward extension of SERS studies to alloys of platinum-group metals. These materials play a decisive role in heterogeneous catalysis and electrocatalysis. In fact, the preparation of SERS-active samples by the classical electrochemical roughening procedure would lead most likely to a preferential dissolution (corrosion) of the less noble element in the alloy, yielding a surface enriched in the more noble component. Nonetheless, the roughening procedure has been shown to be effective in studying the adsorptive properties of bimetallic surfaces prepared by deposition of adatoms of one of the elements on a roughened sample of the second.[40] However, these electrode surfaces may behave differently from bimetallic surfaces created form bulk alloys. In the nanoparticle-on-electrode approach, the alloy particles are prepared in a separate chemical step and their composition is maintained in the actual sample providing SERS. Studies along these lines are currently being developed in our laboratory.

Interestingly, one could envisage the prospect of performing SERS studies on surfaces with well-defined structure. The possibility of tailoring the shapes of the platinum nanoparticles has been demonstrated.[41,42] These nanoparticles with well-defined shape (octahedral, cubic, ...) could be deposited onto a flat electrode surface, which would preserve their shape. If these samples, as expected, are also SERS active, signals coming from adsorbates bonded at surface sites of defined symmetry (depending on the shape of the particles) could be achieved.

Acknowledgment. This work was supported by the Spanish DGI (Ministerio de Ciencia y Tecnología) through projects BQU2003-03737 and BQU2003-03877. We are grateful to the SS.TT.II of the University of Alicante.

References and Notes

(1) Fleishmann, M.; Hendra, P. J.; Mcquillan *Chem. Phys. Lett.* **1974**, *26*, 163.
(2) Campion, A.; Kambhampati, P. *Chem. Soc. Rev.* **1998**, *27*, 241.
(3) Mrozek, M. F.; Weaver, M. J. *J. Am. Chem. Soc.* **2000**, *122*, 150.
(4) Oklejas, V.; Sjostrom, C.; Harris, J. M. *J. Am. Chem. Soc.* **2002**, *124*, 2408.
(5) Shafer-Peltier, K. E.; Haynes, C. L.; Glucksberg, M. R.; Van Duyne, R. P. *J. Am. Chem. Soc.* **2003**, *125*, 588.
(6) Cao, Y. W. C.; Jin, R. C.; Mirkin, C. A. *Science* **2002**, *297*, 1536.
(7) Moskovits, M.; Tay, L.; Yang, J.; Haslett, T. *Top. Appl. Phys.* **2002**, *82*, 215.
(8) Pettinger, M. In *Adsorption of Molecules at Metal Electrodes*; Lipkowski, J., Ross, P. N., Eds.; VCH Publishers: New York, 1992; Chapter 6, p 285.
(9) Vo-Dinh, T. *Trends Anal. Chem.* **1998**, *17*, 557.
(10) (a) Tian, Z. Q.; Ren, B.; Wu, D. Y. *J. Phys. Chem. B* **2002**, *106*, 9463. (b) Tian, Z. Q.; Ren. B. In *Encyclopedia of Electrochemistry*; Bard, A. J., Stratmann, M., Eds.; Wiley-VCH: Weinheim, Germany, 2003; Vol. 3, p 572.
(11) Weaver, M. J. *J. Raman Spectrosc.* **2002**, *33*, 309.
(12) Weaver, M. J. *Adv. Spectrosc.* **1998**, *26*, 219.
(13) Volf, R.; Kral, V.; Hrdlicka, J.; Shishkanova, T. V.; Broncova, G.; Krondak, M.; Grotschelova, S.; St'astny, M.; Kroulik, J.; Valik, M.; Matejka, P.; Volka, K. *Solid State Ionics* **2002**, *154*−*155*, 57−63.
(14) Cooney, R. P.; Fleischmann; Hendra, P. J. *J. Chem. Soc., Chem. Commun.* **1977**, 235.
(15) Bilmes, S. A.; Rubim, J. C.; Otto, A.; Arvía, A. J. *Chem. Phys. Lett.* **1989**, *159*, 89.
(16) (a) Zou, S.; Weaver, M. J. *Anal. Chem.* **1998**, *70*, 2387. (b) Zou, S.; Gómez, R.; Weaver, M. J. *Langmuir* **1997**, *13*, 6713.
(17) Cai, W. B.; Ren, B.; Li, X. Q.; She, C. X.; Liu, F. M.; Cai, X. W.; Tian, Z. Q. *Surf. Sci.* **1998**, *406*, 9.
(18) Ren, B.; Lin, X.-F.; Yang, Z.-L.; Lin, G.-K.; Aroca, R. F.; Mao, B.-W.; Tian, Z.-Q. *J. Am. Chem. Soc.* **2003**, *125*, 9598.
(19) Moskovits, H. *Rev. Mod. Phys.* **1985**, *57*, 783.
(20) Vogel, E.; Kiefer, W.; Deckert, V.; Zeisel, D. *J. Raman Spectrosc.* **1998**, *29*, 693.
(21) Cai, W.; Wan, L.; Noda, H.; Hibino, J.; Ataka, K.; Osawa, M. *Langmuir* **1998**, *14*, 6992.
(22) Makanova, O. V.; Ostafin, A. E.; Miyouhi, H.; Norris, J. R., Jr.; Meisel, D. *J. Phys. Chem. B* **1999**, *103*, 9080.
(23) Creighton, J. A. *Surf. Sci.* **1983**, *124*, 209.
(24) Voisin, C.; Fetti, N. D.; Christofilos, D.; Vallee, F. *J. Phys. Chem. B* **2001**, *105*, 2264.
(25) Litorja, M.; Haynes, C. L.; Haes, A. J.; Jensen, T. R.; Duyne, R. P. V. *J. Phys. Chem. B* **2001**, *105*, 6907.
(26) Klogin, E.; Kreisig, S. M.; Copitzky *Prog. Colloid Polym. Sci.* **1998**, *109*, 232.
(27) Guo, L.; Huang, Q.; Li, X.-Y.; Yang, S. *Phys. Chem. Chem. Phys.* **2001**, *3*, 1661.
(28) Solla-Gullón, J.; Rodes, A.; Montiel, V.; Aldaz, A.; Clavilier, J. *J. Electroanal. Chem.* **2003**, *554*−*555*, 273.
(29) *Catalysis and Electrocatalysis at Nanoparticle Surfaces*; Wieckowski, A., Savinova, E. R., Vayenas, C. G., Eds.; Marcel Dekker: New York, 2003.
(30) Park, S.; Yang, P.; Corredor, P.; Weaver, M. J. *J. Am. Chem. Soc.* **2002**, *124*, 2428.
(31) Yao, J.-L.; Tang, J.; Wu, D.-Y.; Sun, D.-M.; Xue, K.-H.; Ren, B.; Mao, B.-W.; Tian, Z.-Q. *Surf. Sci.* **2002**, *514*, 108.
(32) Solla-Gullón, J.; Montiel, V.; Aldaz, A.; Clavilier, J. *J. Electrochem. Soc.* **2003**, *150*, E104.
(33) Kawashima, Y.; Katagiri, G. *Phys. Rev. B* **1995**, *52*, 10053.
(34) Rubim, J. C.; Corio, P.; Ribeiro, M. C. C.; Matz, M. *J. Phys. Chem.* **1995**, *99*, 15765.
(35) Zou, S.-Z.; Weaver, M. J. *J. Phys. Chem. B* **1996**, *100*, 4237.
(36) Mrozek, M. F.; Xie, Y.; Weaver, M. J. *Anal. Chem.* **2001**, *73*, 5953.
(37) Ren, B.; Xu, X.; Li, X. Q.; Cai, W. B.; Tian, Z. Q. *Surf. Sci.* **1999**, *427*−*428*, 157.
(38) Cai, W. B.; Ren, B.; Liu, F. M.; Li, X. Q.; She, C. X.; Cai, X. W.; Tian, Z. Q. *Surf. Sci.* **1998**, *406*, 9.
(39) Ren, B.; Wu, D.-Y.; Mao, B.-W.; Tian, Z.-Q. *J. Phys. Chem. B* **2003**, *107*, 2752.
(40) She, C.-X.; Xiang, J.; Ren, B.; Zhong, Q.-L.; Wang, X.-C.; Tian, Z.-Q. *J. Korean Electrochem. Soc.* **2002**, *5*, 221.
(41) Ahmadi, T. S.; Wang, Z. L.; Henglein, A.; El-Sayed, M. A. *Chem. Mater.* **1996**, *8*, 1161.
(42) Ahmadi, T. S.; Wang, Z. L.; Green, T. C.; Henglein, A.; El-Sayed, M. A. *Science* **1996**, *272*, 1924.